Article:

Mengoni, M, Ponthot, JP and Boman, R (2016) Mesh management methods in finite element simulations of orthodontic tooth movement. Medical Engineering and Physics, 38 (2). pp. 140-147. ISSN 1350-4533

https://doi.org/10.1016/j.medengphy.2015.11.005

Mesh Management Methods in Finite Element Simulations of Orthodontic Tooth Movement

M. Mengoni[a,*], J.P. Ponthot[a], R. Boman[a]

[a] *University of Liege (ULg), Department of Aerospace and Mechanical Engineering, Non-linear Computational Mechanics (LTAS/MN^{2}L), Liège, Belgium*

Abstract

In finite element simulations of orthodontic tooth movement, one of the challenges is to represent long term tooth movement. Large deformation of the periodontal ligament and large tooth displacment due to bone remodelling lead to large distortions of the finite element mesh when a Lagrangian formalism is used. We propose in this work to use an Arbitrary Lagrangian Eulerian (ALE) formalism to delay remeshing operations. A large tooth displacement is obtained including effect of remodelling without the need of remeshing steps but keeping a good-quality mesh. Very large deformations in soft tissues such as the periodontal ligament is obtained using a combination of the ALE formalism used continuously and a remeshing algorithm used when needed. This work demonstrates that the ALE formalism is a very efficient way to delay remeshing operations.

Keywords: Orthodontic Tooth Movement, Arbitrary Lagrangian Eulerian formalism, Remeshing, Finite Element Method

Word count: 3706

---

*Corresponding author.

Email address: `m.mengoni@leeds.ac.uk` (M. Mengoni)

1. Introduction

The Finite Element (FE) Method is a numerical procedure to approximate problems modelled by partial differential equations using a discrete representation of the problem to be solved on a grid of nodes and elements. In mechanical models, it involves procedures to calculate in each element stresses and strains resulting from external factors such as forces and displacements. The FE method is extremely useful for estimating mechanical response of biomaterials and tissues that can hardly be measured in vivo. It has been used in dentistry-related problems since the 1970's, as reviewed in [1, 2, 3], with the interest of determining stresses in dental structures and materials used for clinical treatment and repair, and to improve the strength and response of these treatments, procedures and associated adaptive behaviour of the tissues. In particular, for orthodontic tooth movement problems, the FE method can deliver not only the global mechanical behaviour of the involved structures, i.e. the tooth mobility, but also it gives access to local stresses and strains of each tissue. That local behaviour is essential to couple mechanics and biology and to model the adaptive response of tissues.

One of the main principles of orthodontic treatment is to impose external loads to a tooth, leading to an altered mechanical environment in the periodontal ligament (PDL) surrounding the tooth and bone tissues supporting it. This altered environment induces remodelling and leads the tooth into a new position. The driving force of remodelling is the biological interaction between bone tissues and the PDL. Remodelling models in orthodontics FE analysis usually involve an update of the purely mechanical displacement of the tooth due to applied forces by a displacement due to the remodelling stimulus [4, 5]. The stimulus for remodelling is either the strain energy density [6], based on the strain field [7, 8, 9], or based on the stress field [10]. However, other approaches can also be found: Soncini and Pietrabissa [11] or van Schepdael et al. [12] proposed remodelling models considering a viscous behaviour of the bone (viscoelastic Maxwell models) ; Cronau et al. [13] proposed a remodelling model considering a viscous behaviour of the PDL (viscoelastic Maxwell model) ; finally, Field et al. [14], Lin et al. [15], Mengoni and Ponthot [16] proposed remodelling laws involving an explicit local change of the bone elastic properties based on the strain level, similarly to remodelling algorithms used within the orthopaedic biomechanics literature.

In any case, due to remodelling and therefore softening of the bone tissue, or when the PDL deformations are physically modelled, large deformations are locally encountered during tooth movement. This leads to deformations of the finite element mesh up to a point where the mesh quality is no longer sufficient enough either to continue the computation, if elements happen to get highly distorted, or simply to blindly trust the solution quality. To overcome this problem, mesh management techniques such as the Arbitrary Lagrangian-Eulerian (ALE) formalism and a remeshing method are proposed in this work. The ALE formalism decouples, at each time step of the simulation, the mesh movement from the material displacement. The remeshing method authorises, at given predefined time step, a complete remesh the deformed geometry. The ALE method has been previously used in biomechanical problems, specifically in cardiovascular problems where fluid-structure interactions between blood flow and natural tissues [17, 18, 19, 20, 21, 22, 23] or devices [24, 25, 26] are modelled, or in deformation problems of soft organs such as breasts and lungs [27, 28], or in car safety simulation such as airbag deployment [29]. However, to the best of the authors' knowledge, it has not been used with dentistry-related models. Remeshing methods are often used in bone remodelling models when remodelling algorithms involve the computation of a new geometry [5] rather than being embedded into the constitutive behaviour of the tissue. In the present study, the remodelling algorithm for orthodontic tooth movement [16] is embedded into the bone tissue behaviour allowing it to soften as biological activity occurs. The aim of this study was to assess the advantages and drawbacks of using the ALE method and remeshing procedures to model a tooth moving along a finite distance in the alveolar bone due to orthodontic forces. The simulations presented in this work were performed using the non-linear implicit FE code METAFOR (developed at the LTAS/MN^{2}L, University of Liège, Belgium - metafor.ltas.ulg.ac.be). All material models [16, 30] and numerical methods such as ALE [31, 32] and remeshing method [33] used in this work were previously implemented, verified, or validated, in this software in such a way that they are fully compatible. They are here used in the new context of long term orthodontic tooth movement. Similar simulations would have been difficult in traditional commercial software.

2. Methods

2.1. Theoretical Background

The Arbitrary Lagrangian Eulerian (ALE) formalism [34] consists in decoupling the movement of the finite element mesh from the deformations of the underlying material. Compared to the classical Lagrangian formalism where the nodes follow the same material particles or to the Eulerian formalism where the nodes are fixed in space, the motion of the ALE computational grid can be arbitrarily chosen by the user of the FE code. ALE methods are very helpful in large deformation problems, such as the applications presented in this paper, when the quality of the finite elements deteriorates rapidly during the simulation. For these particular models, the quality of the ALE mesh is constantly optimised and costly remeshing operations are delayed, and sometimes completely avoided. Another kind of problems targeted by ALE methods is the simulation of complex material flows involving free boundaries which cannot be handled by the traditional Eulerian formalism with a fixed mesh [31].

The ALE equilibrium equations contain two sets of unknowns defined at each node [34]: the material velocity and the mesh velocity. This system of equations must be completed with additional relationships describing the motion of the mesh. However, in the case of highly nonlinear problems including large deformations and possibly contact between boundaries, writing these equations explicitly is very difficult. The common workaround is to solve the two sets of equations sequentially with an operator split procedure. At each time-step, the nonlinear equilibrium equations are iteratively solved as in the Lagrangian case, i.e. with a mesh that follows the material. Once the equilibrium is reached, the nodes are then relocated using appropriate techniques [31] such as smoothing, projections or prescribed displacements. The solution fields (e.g. the stress tensor and the internal variables of the material) are eventually transferred from the old mesh configuration to the new one. Since the topology of both meshes is exactly the same (each element keeps the same neighbours during the redefinition of the new mesh) and the distance between two corresponding elements is usually small, very fast and efficient transfer algorithms based on projections and the Finite Volume Method can be employed [32, 35, 36].

When the deformation of the computational domain becomes so important that the quality of the mesh cannot be improved without modifying its topology, a new one has to be generated by a remeshing procedure. In METAFOR, this expensive operation consists in several steps. First the boundaries of the deformed domain are extracted and converted to smooth cubic splines which are remeshed one by one using a prescribed mesh density. Secondly the interior of the domain is remeshed thanks to a robust quadrangular mesher [37]. Then the solution fields are transferred from the old mesh to the new one. The transfer methods used in this work [33] are very similar to the former ones implemented in the ALE context. Nevertheless, they are much slower because the projection requires the determination of all the elements of the old mesh which intersects each element of the new mesh. In the ALE case, this expensive search can be restricted to the element itself and its direct neighbours. At last, when all the fields have been transferred, the time integration procedure is restarted with the new mesh using the ALE formalism until a new remeshing operation is required.

In the current state of the code, remeshing operations should be manually planned by the user. However, thanks to the ALE formalism which constantly improves the mesh quality despite of large deformations, the number of remeshing is expected to be much lower than in a purely Lagrangian approach.

2.2. Modelling of Orthodontic Tooth Movement

Two types of simulations were developed to illustrate the need for mesh management methods in finite element models of orthodontic tooth movements. Both simulations are 2D plane-strain models.

The first simulation was an academic case, testing the capacity of a remodelling model combined with mesh management methods for tooth movement applications. A 2D single-rooted tooth was modelled with a root thickness of 7 mm at the alveolar margin and a root height of 16 mm, surrounded by alveolar bone (composed solely of trabecular tissue) 49-mm thick on each side of the tooth, and 40-mm high (see Figure 1). This model corresponded to a simulation of a tooth moving along the alveolar arch, with no other teeth present. The size of the considered bone reduced boundary effects to which remodelling algorithms are very sensitive [38, 39]. The tooth was considered as being a rigid tissue and the PDL was represented with a piecewise-linear interface model [16]. The bone was assumed to follow mechanical and remodelling constitutive models such as described in [16, 30] with an initial uniform bone density of 1.3 gr/cc. These material and remodelling models assumed an anisotropic elastoplastic bone, submitted to remodelling in such a way that bone formation was observed at high strain energy density locations and bone resorption at low strain energy density locations. The coupling between the constitutive model and the remodelling model was expressed in a Continuum Damage Mechanics framework, with a remodelling criterion function of the strain energy density. Bone remodelling followed the concept of the mechanostat theory [40]: the bone density and orientation evolved according to the signed difference between the remodelling criterion and an homeostatic level of that value. All material and remodelling parameters are listed in Table 1. The remodelling rates are the only drivers of time in the remodelling algorithm and the all simulation. All time measures are thus described with respect to arbitrary time units, T. The bone was meshed with linear quadrangular elements using a structured mesh away from the tooth root in the regions delimited by the lateral rectangles $ABHG$ and $EFLK$ and using an unstructured mesh matching the root shape in its surrounding in the region delimited by the central rectangle $BEKH$ (see Figure 1) with a total of 1004 elements. This subdivision of the geometrical domain facilitated the mesh refinement in the area submitted to large strains around the apex of the tooth root. Boundary conditions were applied to represent the outcome of an orthodontic treatment at constant velocity. Boundary conditions representative of a end-of-treatment state, i.e. constant rate of displacement, were applied to the tooth. The tooth root was horizontally translated at a constant velocity to achieve a displacement of 1.5 times its width over 365 units of time. Rigid boundary conditions were applied to the bone basal line while it was restrained vertically on its top line and horizontally on its vertical extremities (see Figure 1). The ALE mesh movement was specified following the tooth kinematics to keep a good mesh quality along the displacement. The unstructured central mesh was moved with the same velocity as the tooth, imposing that the displacement of nodes B, H, and I was identical to that of node C in contact with the tooth root. In the same way, the displacement of nodes E, J, and K was identical to that of node D. The mesh nodes along the root surface (green curve in Figure 1) were relocated using spline curves [31]. Finally, the nodes of lines BC, DE, EK, KJ,

Table 1: Material and Remodelling parameters of tissues

Bone remodelling parameters (model 1 only) [16]

homeostatic stimulus (MPa)	remodelling rate in resorption (μ m/(MPa T))	remodelling rate in formation (μ m/(MPa T))	width of lazy zone (MPa)	degree of anisotropy (-)
0	10	5	0.1	1

Elastoplastic parameters

Material	Young's modulus (GPa)	Poisson's ratio (-)	Yield stress (MPa)	Hardening parameter (MPa)	Apparent density (gr/cc)
Bone	13.75	0.3	200.0	723.7	1.3
Tooth (model 2 only)	19	0.3	-	-	2.7
PDL	piecewise linear (table 2, Figure 2)	0.49	-	-	0.1

JI, IH, and HB were repositioned so that the lines remained straight during the material displacement. All the other inner nodes of the central region were repositioned using Giuliani's smoothing method [41], which is based on an iterative optimisation of the shape of neighbouring elements. The two structured regions (sections $ABHG$ and $EFLK$) were meshed using a transfinite mesher. After relocation of the nodes, the different internal fields were transferred onto the new mesh with a first order Godunov scheme [36, 32].

The second, more realistic, simulation consisted in a 2D lower incisor submitted to loading representative of clinical treatment. A mandible geometry was obtained from the INRIA/GAMMA repository [52], constructed from a

	Engineering Strain	Tangential Modulus
	[-]	[MPa]
Compression	0.0	0.068 (i.e. Young's modulus)
	$0.0 \rightarrow -0.25$	linear variation up to 0.68
	$-0.25 \rightarrow -0.31$	linear variation up to 8.5
	$-0.31 \rightarrow -0.82$	constant value of 8.5
	< -0.82	13.5
Traction	0.0	0.068 (i.e. Young's modulus)
	$0.0 \rightarrow 0.14$	linear variation up to 1.35
	$0.14 \rightarrow 0.63$	constant value of 8.5
	> 0.63	0.01

Table 2: Values of the mechanical model for the periodontal ligament

surface reconstruction of the mandibular bone and its teeth. The 2D outline in the mesiodistal plane of the left central incisor was extracted. The PDL was created at the interface between the bone and the tooth assuming a constant thickness of 0.2 mm (see Figure 3). The three surfaces (PDL, tooth, and alveolar bone) were meshed with linear quadrangular elements. The resulting unstructured mesh was composed of 1000 elements for the PDL, 1820 for the alveolar bone, and 2294 for the tooth. The tooth and bone were modelled with a linear elastic constitutive law. The PDL was represented with a piecewise-linear elastic material (see Table 2, Figure 2). Only the initial tooth displacement was modelled and no remodelling algorithm was used. All material parameters are listed in Table 1. Boundary conditions were applied to represent the outcome of a constant-force orthodontic treatment. The bone was clamped on its basal line (see Figure 3, red curve). A pressure representative of a total 1.2 N force was gradually applied on the labial side of the tooth crown (see Figure 3). The force used in this model can be classified as a high orthodontic force. The PDL was thus submitted to large strains and the numerical convergence could not be ensured with a classical Lagrangian approach due to excessive mesh distortion. Therefore, two mesh management techniques were used: the Arbitrary Lagrangian-Eulerian (ALE) method and a remeshing technique. The ALE method was applied at each time increment of the simulation while remeshing was applied at four load levels of 0.65 N, 0.85 N , 0.95 N and 1.05 N. Those loads were determined in a pre-analysis as the values for which the ALE formalism could not manage the large deformations. In the case of the PDL, a spline rezoner [31] was used for the two free boundaries delimiting the surface of the PDL (purple lines in Figure 3). It permitted to relocate the nodes of the PDL boundary with a cubic spline. Guiliani's iterative smoothing method was subsequently used on the inner nodes of the mesh, homogenizing the elements area [41]. After repositioning of the nodes, the different internal fields were transferred onto the new mesh using a first order Godunov scheme [36, 32]. When the ALE rezoning was not sufficient to keep a good mesh quality, a full remeshing of the deformed geometry was considered. In this case, cubic splines were built on the outline of the deformed geometry which was fully remeshed [53]. Solution fields were transferred from the old mesh to the new mesh using a projection technique [33].

3. Results

The benefit of the ALE method in the first model was analysed comparing the remodelling criteria values at 50% of the maximal displacement, i.e. 5.25 mm (see Figure 4) with and without ALE. At that level of displacement, both methods showed the same results in the regions where the mesh is of good quality. However, the classical Lagrangian method produced a distorted mesh around the tooth apex to a point where the local numerical solution could not be trusted any more, with a remodelling criterion reaching high values around the tooth apex. Displacement higher than 5.4 mm could not be computed with a Lagrangian mesh due to negative jacobians while the ALE mesh allowed the full tooth displacement to be computed. The force needed for the ALE model (Figure 5 plain line) is the same as the one needed for the Lagrangian model (Figure 5 dash-dot line) where the Lagrangian mesh is of good quality (for the first 2.6 mm of translation). The Lagrangian force however deviates from the ALE one when the mesh becomes too distorted. The remodelling constitutive model facilitated the tooth movement, requiring a force about 40% lower than the force needed to displace the tooth of the same length if no biological remodelling were present (Figure 5). The ALE mesh kinematics is depicted in Figure 6 were the remodelling criterion is plotted at three different time points of the simulation. The unstructured mesh around the tooth in the rectangle $BEKH$ of Figure 1 followed the tooth movement. The structured mesh of the upstream rectangle $ABHG$ expanded as the tooth moved away from the fixed left boundary while the structured mesh of the downstream rectangle $EFLK$ shrunk.

The forces applied on the second model led to large strains around the tooth collar. The soft PDL thus deformed up to a point where the mesh quality can not be trusted any more (see Figure 7(b)). A better representation of the large strains at the alveolar margin without excessive mesh distortion was allowed by the ALE method (see initial and deformed meshes, with and without ALE in Figure 7(a-d)). A tipping force of 0.65 N was applied while keeping a good mesh quality but a higher force could not be used, with elements too distorted for a higher force, whatever the ALE node relocation algorithm used (Figure 7(e), red element). Indeed in the cervical area, because of the almost incompressible behaviour of the ligament, the free boundaries created convex and concave menisci so that inversion of the finite elements occured. The first load step defined for remeshing was when the applied load reached 0.65 N. The resulting new mesh (Figure 8(b)) allowed the computation to continue further (still applying the ALE method at each time step) up to a 0.85 N force. At a higher force level the mesh became once more too distorted on the tension side (Figure 8(c)). New remeshing instants were defined similarly at 0.85 N, 0.95 N, and 1.05 N. This fourth and final mesh was used for forces up to 1.2 N. This remeshing technique could be used further, every time defining new time steps at which remeshing takes place. The displacement of the tooth tip was identical for all three models (purely Lagrangian, ALE, ALE with remeshing) as long as the model converged (see Figure 9).

4. Discussion

This work proposes an assessment of computational tools such as the Arbitrary Lagrangian Eulerian formalism and remeshing in the development of orthodontics tooth movement predictive models. Although this work focuses on the computational methods and the presented models are not validated against experimental and clinical data, it demonstrates the advantages and drawbacks of these methods for soft tissues modelling and remodelling models.

The first model shows that the ALE formalism makes it possible to reach a large displacement of a tooth within a mandible including the effect of bone remodelling without any remeshing steps. While the model is not representative of an actual tooth movement, it emphasizes the need to keep a good-quality mesh where remodelling is observed so that the bone formation or resorption is not artifically modified by numerical errors due to excessive mesh distortion. It should be emphasized that the aim of the proposed model is not clinically-driven. While the loading conditions have been chosen to represent average constant rate of displacement achieved in the third phase of orthodontic treatments [54, 55], the reproduced movement is not a model of an actual treatment. In particular, no physiological homeostatic loads are present, and the constant velocity condition is assumed to be the result of using orthodontic devices which are not modelled. It is unlikely that a constant rate of displacement would be achieved over such a distance without the need to adapt the device used.

The second model underlines the possibility of reaching very large deformations in soft tissues models. The combination of the ALE formalism used continuously throughout the simulation with a remeshing algorithm used when needed facilitates the development of a reliable model of the menisci creation at the free boundaries of thin soft tissues. Analysing the evolution of the mesh in the periodontal ligament however shows that the number of elements describing those boundaries has to decrease with increasing applied load. The creation of the menisci due to the deformation needs an initial fine mesh. Once the menisci are formed, building a fine mesh without creating badly shaped elements at the extremities is very hard. At the tension side, the angle between the concave meniscus and the tooth boundary increases as the force increases, and become obtuse. At the compression side however, the angle between the convex meniscus and the bone boundary decreases, with a tendency to deform the quadrangles into triangles. Therefore, the description of the geometry of the free boundary is less and less accurate in order to be able to mesh it properly. Using the combination of ALE and remeshing methods in this case allows the simulation to reach force levels that are representative of orthodontic treatment force levels. This is a major improvement with respect to a purely Lagrangian approach that can only reach a force a quarter of the final value achieved here.

3D models of a set of adjacent teeth submitted to loading through orthodontic devices would however better represent an actual clincal outcome. Such models have already shown to perform well in initial tooth movement predictions and in long-term prediction when the remodelling algorithm involves full remeshing of a new geometry at each time step. In the case of remodelling algorithm such as used in this work, the presented applications demonstrate that the ALE formalism is a very efficient way to delay remeshing operations. The later are usually very expensive in terms of CPU time and user work time, even for 2D problems. In a 3D context, remeshing becomes a major issue and we think that it could be partially solved by the

ALE methods, which are already fully functional in 3D. Applications in 3D will be thus addressed in a near future.

This computational work presents a promising approach to model large tooth displacements in orthodontic treatment. This approach is not limited to orthodontic treatment and can be used in combination with any remodelling algorithm fully embedded within the constitutive law and not needing full computation of a new geometry.

5. Author's declarations

Funding: None declared

Conflicts of Interest: None declared

Ethical Approval: Not required

References

[1] Cattaneo PM, Dalstra M, Melsen B. The finite element method : a tool to study orthodontic tooth movement. J Dent Res 2005;84(5):428–33.

[2] Mackerle J. Finite element modelling and simulations in dentistry: a bibliography 1990-2003. Comput Methods Biomech Biomed Engin 2004;7(5):277–303.

[3] Van Staden RC, Guan H, Loo YC. Application of the finite element method in dental implant research. Comput Methods Biomech Biomed Engin 2006;9(4):257–70.

[4] Provatidis CG. A bone-remodelling scheme based on principal strains applied to a tooth during translation. Comput Methods Biomech Biomed Engin 2003;6(5-6):347–52.

[5] Chen J, Li W, Swain MV, Ali Darendeliler M, Li Q. A periodontal ligament driven remodeling algorithm for orthodontic tooth movement. J Biomech 2014;47(7):1689–95.

[6] Li J, Li H, Shi L, Fok AS, Ucer C, Devlin H, et al. A mathematical model for simulating the bone remodeling process under mechanical stimulus. Dent Mater 2007;23(9):1073–8.

[7] Bourauel C, Vollmer D, Jäger A. Application of bone remodeling theories in the simulation of orthodontic tooth movements. J Orofac Orthop 2000;61(4):266–79.

[8] Marangalou JH, Ghalichi F, Mirzakouchaki B. Numerical simulation of orthodontic bone remodeling. Orthod Waves 2009;68(2):64–71.

[9] Qian Y, Fan Y, Liu Z, Zhang M. Numerical simulation of tooth movement in a therapy period. Clin Biomech 2008;23(Supplement 1):S48–52.

[10] Kojima Y, Kawamura J, Fukui H. Finite element analysis of the effect of force directions on tooth movement in extraction space closure with miniscrew sliding mechanics. Am J Orthod Dentofacial Orthop 2012;142(4):501–8.

[11] Soncini M, Pietrabissa R. Quantitative approach for the prediction of tooth movement during orthodontic treatment. Comput Methods Biomech Biomed Engin 2002;5(5):361–8.

[12] van Schepdael A, De Bondt K, Geris L, Sloten JV. A visco-elastic model for the prediction of orthodontic tooth movement. Comput Methods Biomech Biomed Engin 2014;17(6):581–90.

[13] Cronau M, Ihlow D, Kubein-Meesenburg D, Fanghnel J, Dathe H, Ngerl H. Biomechanical features of the periodontium: an experimental pilot study in vivo. Am J Orthod Dentofacial Orthop 2006;129(5):599.e13–21.

[14] Field C, Li Q, Li W, Thompson M, Swain M. A comparative mechanical and bone remodelling study of all-ceramic posterior inlay and onlay fixed partial dentures. J Dent 2012;40(1):48–56.

[15] Lin D, Li Q, Li W, Duckmanton N, Swain M. Mandibular bone remodeling induced by dental implant. J Biomech 2010;43(2):287–93.

[16] Mengoni M, Ponthot JP. A generic anisotropic continuum damage model integration scheme adaptable to both ductile damage and biological damage-like situations. Int J Plasticity 2015;66:46–70.

[17] Colciago C, Deparis S, Quarteroni A. Comparisons between reduced order models and full 3D models for fluid-structure interaction problems in haemodynamics. J Comput Appl Math 2014;265:120–38.

[18] Martino ED, Guadagni G, Fumero A, Ballerini G, Spirito R, Biglioli P, et al. Fluid-structure interaction within realistic three-dimensional models of the aneurysmatic aorta as a guidance to assess the risk of rupture of the aneurysm. Med Eng Phys 2001;23(9):647–55.

[19] Javadzadegan A, Fakhim B, Behnia M, Behnia M. Fluid-structure interaction investigation of spiral flow in a model of abdominal aortic aneurysm. Eur J Mech B Fluids 2014;46:109–17.

[20] Langer U, Yang H. Partitioned solution algorithms for fluid-structure interaction problems with hyperelastic models. J Comput Appl Math 2015;276:47–61.

[21] Lee C, Zhang Y, Takao H, Murayama Y, Qian Y. A fluid-structure interaction study using patient-specific ruptured and unruptured aneurysm: The effect of aneurysm morphology, hypertension and elasticity. J Biomech 2013;46(14):2402–10.

[22] Taelman L, Degroote J, Swillens A, Vierendeels J, Segers P. Fluid-structure interaction simulation of pulse propagation in arteries: Numerical pitfalls and hemodynamic impact of a local stiffening. Int J Eng Sci 2014;77:1–13.

[23] Wolters B, Rutten M, Schurink G, Kose U, de Hart J, van de Vosse F. A patient-specific computational model of fluid-structure interaction in abdominal aortic aneurysms. Med Eng Phys 2005;27(10):871–83.

[24] Chiastra C, Migliavacca F, Martínez MÁ, Malvè M. On the necessity of modelling fluid-structure interaction for stented coronary arteries. J Mech Behav Biomed Mater 2014;34:217–30.

[25] Guivier-Curien C, Deplano V, Bertrand E. Validation of a numerical 3D fluid-structure interaction model for a prosthetic valve based on experimental PIV measurements. Med Eng Phys 2009;31(8):986–93.

[26] McCormick M, Nordsletten D, Kay D, Smith N. Simulating left ventricular fluid-solid mechanics through the cardiac cycle under LVAD support. J Comput Phys 2013;244:80–96.

[27] Yin Y, Choi J, Hoffman EA, Tawhai MH, Lin CL. A multiscale MDCT image-based breathing lung model with time-varying regional ventilation. J Comput Phys 2013;244:168–92.

[28] Kuhlmann M, Fear E, Ramirez-Serrano A, Federico S. Mechanical model of the breast for the prediction of deformation during imaging. Med Eng Phys 2013;35(4):470–8.

[29] Potula S, Solanki K, Oglesby D, Tschopp M, Bhatia M. Investigating occupant safety through simulating the interaction between side curtain airbag deployment and an out-of-position occupant. Accid Anal Prev 2012;49:392–403.

[30] Mengoni M, Ponthot JP. An enhanced version of a bone remodelling model based on the continuum damage mechanics theory. Comput Methods Biomech Biomed Engin 2015;18(12):1367–76.

[31] Boman R, Ponthot JP. Efficient ALE mesh management for 3D quasi-Eulerian problems. Int J Numer Methods Eng 2012;92(10):857–90.

[32] Boman R, Ponthot JP. Enhanced ALE data transfer strategy for explicit and implicit thermomechanical simulations of high-speed processes. Int J Impact Eng 2013;53:62–73.

[33] Bussetta P, Boman R, Ponthot JP. Efficient 3D data transfer operators

based on numerical integration. Int J Numer Methods Eng 2015;102(3-4):892–929.

[34] Donéa J, Huerta A, Ponthot JP, Rodriguez-Ferran A. Encyclopedia of Computational Mechanics, Volume 1; chap. 14: Arbitrary Lagrangian-Eulerian Methods. Stein, E. and de Borst, R. and Hughes T. J. R.; 2004, p. 413–37.

[35] Benson DJ. An efficient, accurate, simple ALE method for non-linear finite element programs. Comput Methods Appl Mech Eng 1989;72(3):305–50.

[36] Rodriguez-Ferran A, Casadei F, Huerta A. ALE stress update for transient and quasistatic processes. Int J Numer Methods Eng 1998;42:241–62.

[37] Sarrate J, Huerta A. Efficient unstructured quadrilateral mesh generation. Int J Numer Methods Eng 2000;49:1327–50.

[38] Bitsakos C, Kerner J, Fisher I, Amis AA. The effect of muscle loading on the simulation of bone remodelling in the proximal femur. J Biomech 2005;38(1):133–9.

[39] Fernández J, García-Aznar J, Martínez R. Numerical analysis of a diffusive strain-adaptive bone remodelling theory. Int J Solids Struct 2012;49(15):2085–93.

[40] Frost H. Skeletal structural adaptations to mechanical usage (SATMU): 2. Redefining Wolff's law: the remodeling problem. Anat Rec 1990;226(4):414–22.

[41] Giuliani S. An algorithm for continuous rezoning of the hydrodynamic grid in Arbitrary Lagrangian-Eulerian computer codes. Nucl Eng Des 1982;72(2):205–12.

[42] Dorow C, Krstin N, Sander FG. Determination of the mechanical properties of the periodontal ligament in a uniaxial tensional experiment. J Orofac Orthop 2003;64(2):100–7.

[43] Natali AN, Carniel EL, Pavan PG, Bourauel C, Ziegler A, Keilig L. Experimental-numerical analysis of minipig's multi-rooted teeth. J Biomech 2007;40(8):1701–8.

[44] Natali AN, Pavan PG, Carniel EL, Dorow C. A transversally isotropic elasto-damage constitutive model for the periodontal ligament. Comput Methods Biomech Biomed Engin 2003;6(5-6):pp. 329–336.

[45] Aversa R, Apicella D, Perillo L, Sorrentino R, Zarone F, Ferrari M, et al. Non-linear elastic three-dimensional finite element analysis on the effect of endocrown material rigidity on alveolar bone remodeling process. Dent Mater 2009;25(5):678–90.

[46] Pini M, Wiskott HWA, Scherrer SS, Botsis J, Belser UC. Mechanical characterization of bovine periodontal ligament. J Periodontal Res 2002;37(4):237–44.

[47] Pini M, Zysset PK, Botsis J, Contro R. Tensile and compressive behaviour of the bovine periodontal ligament. J Biomech 2004;37(1):111–9.

[48] Toms SR, Eberhardt AW. A nonlinear finite element analysis of the periodontal ligament under orthodontic tooth loading. Am J Orthod Dentofacial Orthop 2003;123(6):657–65.

[49] Komatsu K, Sanctuary C, Shibata T, Shimada A, Botsis J. Stress-relaxation and microscopic dynamics of rabbit periodontal ligament. J Biomech 2007;40(3):634–44.

[50] Borák L, Florian Z, Bartáková S, Prachár P, Murakami N, Ona M, et al. Bilinear elastic property of the periodontal ligament for simulation using a finite element mandible model. Dent Mater J 2011;30(4):448–54.

[51] Qian L, Todo M, Morita Y, Matsushita Y, Koyano K. Deformation analysis of the periodontium considering the viscoelasticity of the periodontal ligament. Dent Mater 2009;25(10):1285–92.

[52] INRIA . Gamma repository. https://www.rocq.inria.fr/gamma/gamma/download/affichage.php?dir=ANATOMY&name=mandibule; last visit 10/2014.

[53] Bussetta P, Dialami N, Boman R, Chiumenti M, Agelet de Saracibar C, Cervera M, et al. Comparison of a fluid and a solid approach for the numerical simulation of friction stir welding with a non-cylindrical pin. Steel Res Int 2014;85(6):968–79.

[54] Buschang PH, Campbell PM, Ruso S. Accelerating tooth movement with corticotomies: is it possible and desirable? Semin Orthod 2012;18(4):286–94.

[55] Dixon V, Read M, O'Brien K, Worthington H, Mandall N. A randomized clinical trial to compare three methods of orthodontic space closure. J Orthod 2002;29(1):31–6.

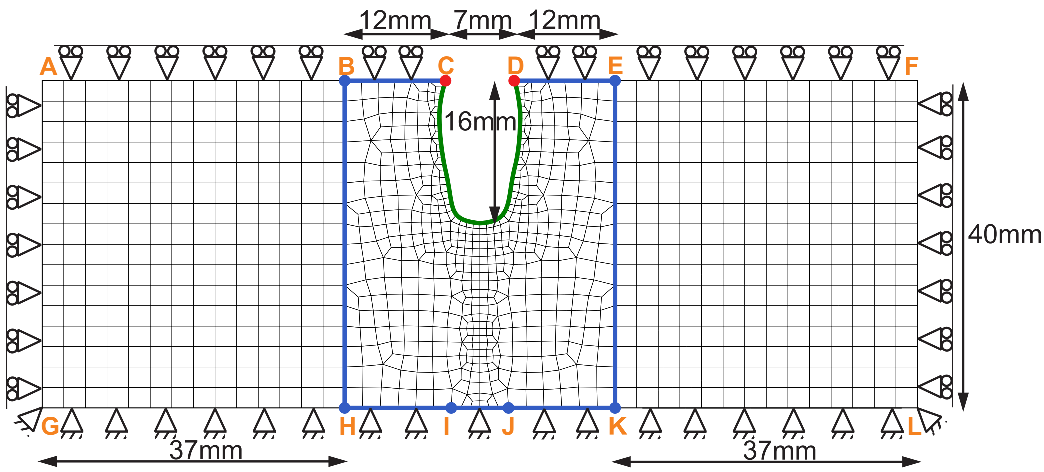

Figure 1: Academic case: geometry, mesh, and ALE mesh management: the nodes on the green curve are relocated using spline curves, the blue points have an horizontal displacement which is set equal to the one of the red points, the blue lines are remeshed (with a constant number of elements) as if they remained straight between their extremities.

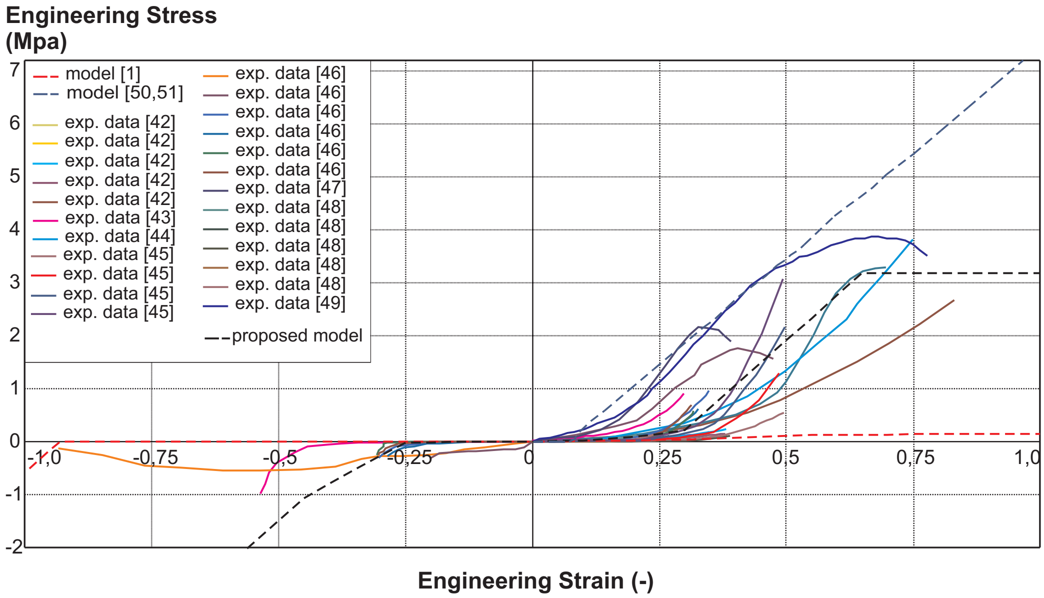

Figure 2: Periodontal Ligament - experimental data [42, 43, 44, 45, 46, 47, 48, 49] : Engineering Strain vs. Engineering Stress for uniaxial tests. The data is labelled after the name of first author of the paper it comes from, followed by the year of publication and the number of the figure in the paper (a letter is added if several curves appear on the same figure). As a comparison, in blue and red dashed line, two multi-linear models [1, 50, 51] that surround this experimental data. In black dashed line, the model used in this work.

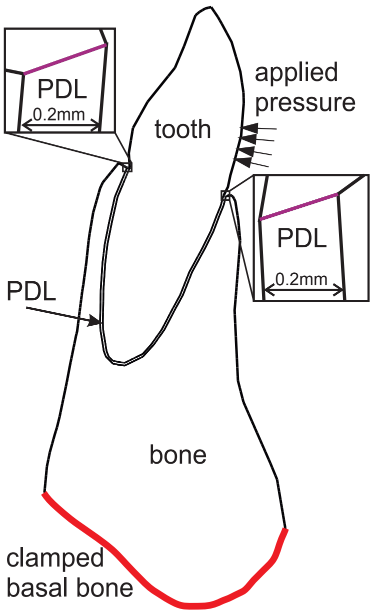

Figure 3: 2D geometry in the mesiodistal plane of the left central incisor.

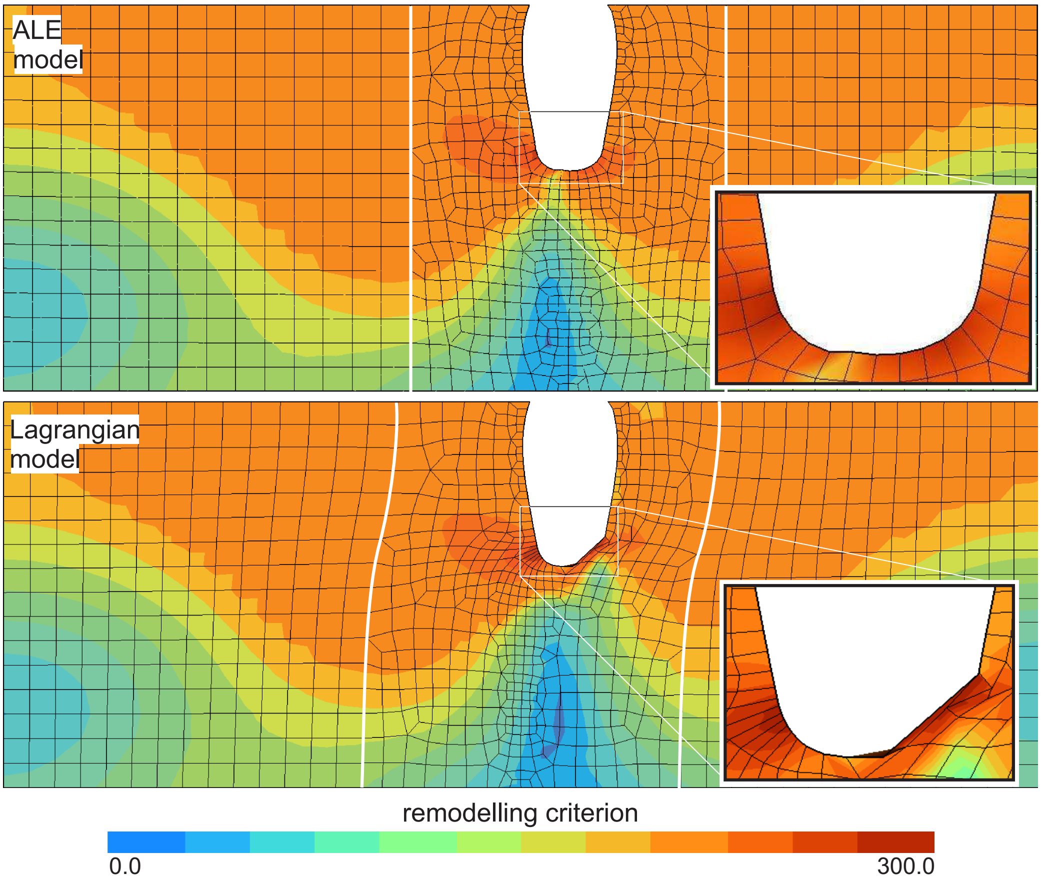

Figure 4: Comparison of the ALE and Lagrangian methods after 180 time units. Top panel: ALE mesh, bottom panel: Lagrangian mesh.

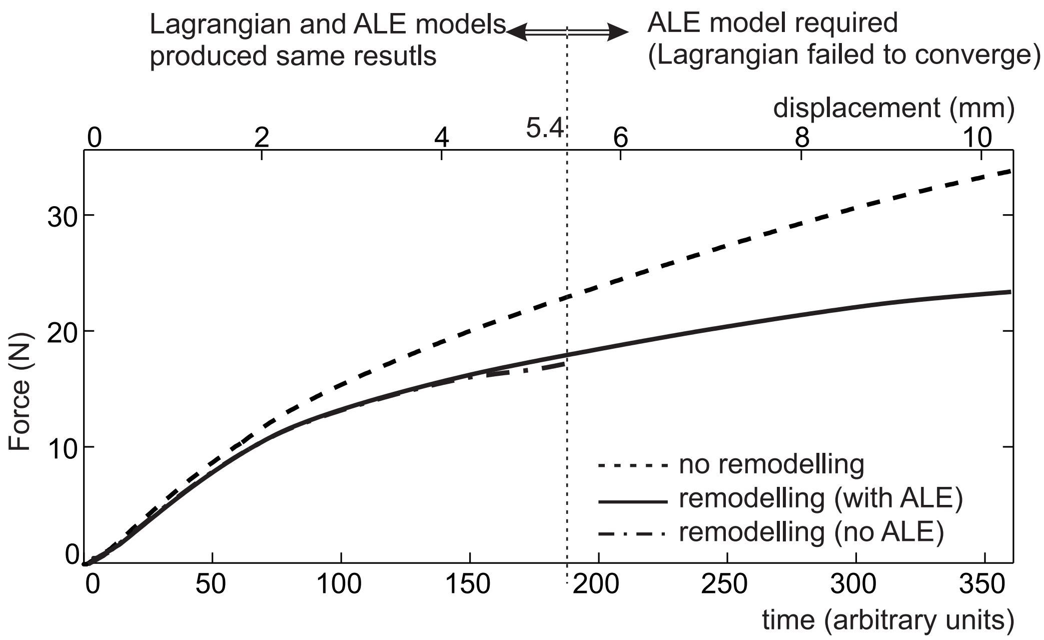

Figure 5: Force vs. time and corresponding displacements for the imposed velocity.

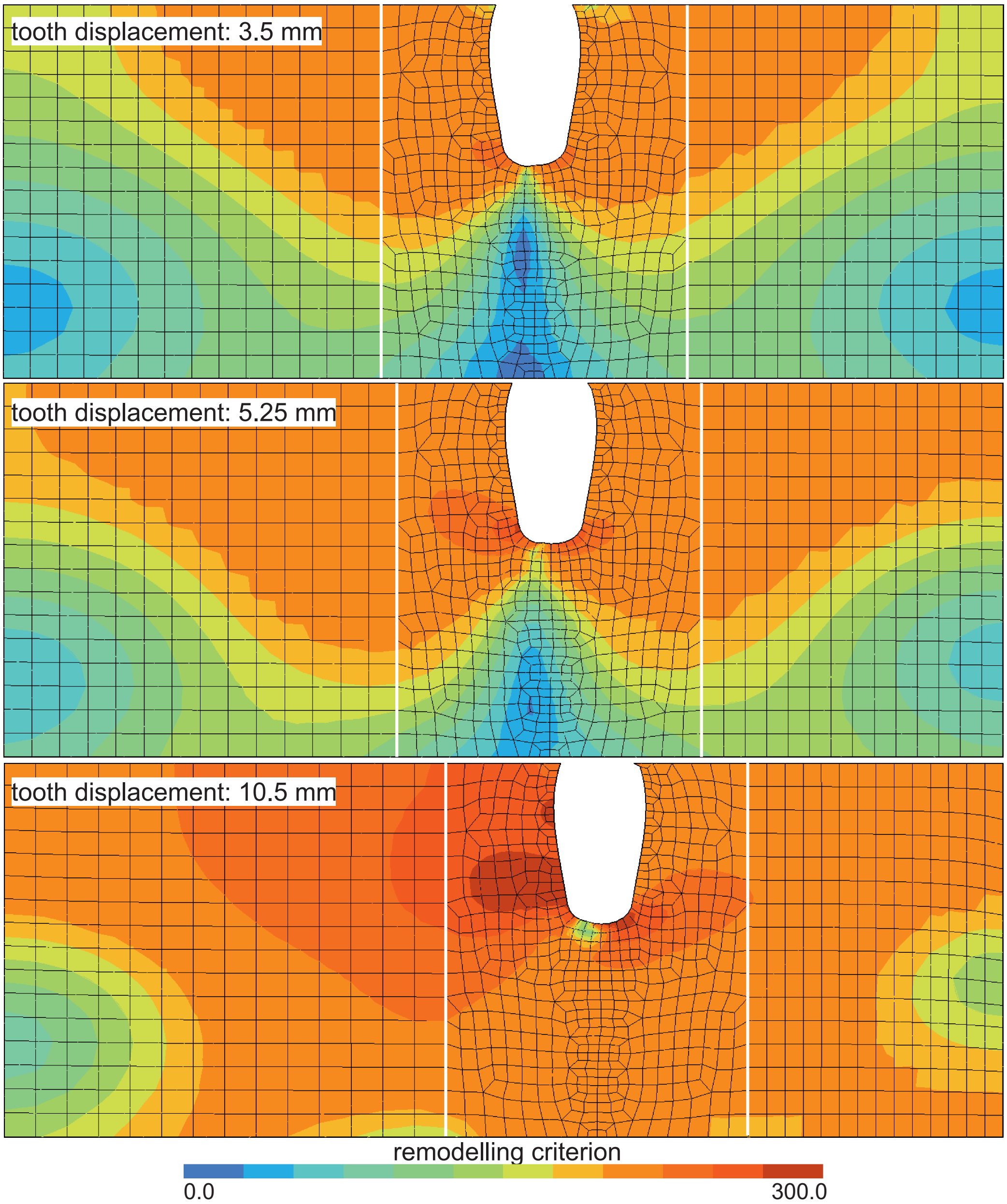

Figure 6: ALE mesh movement: the mesh follows the movement of the tooth.

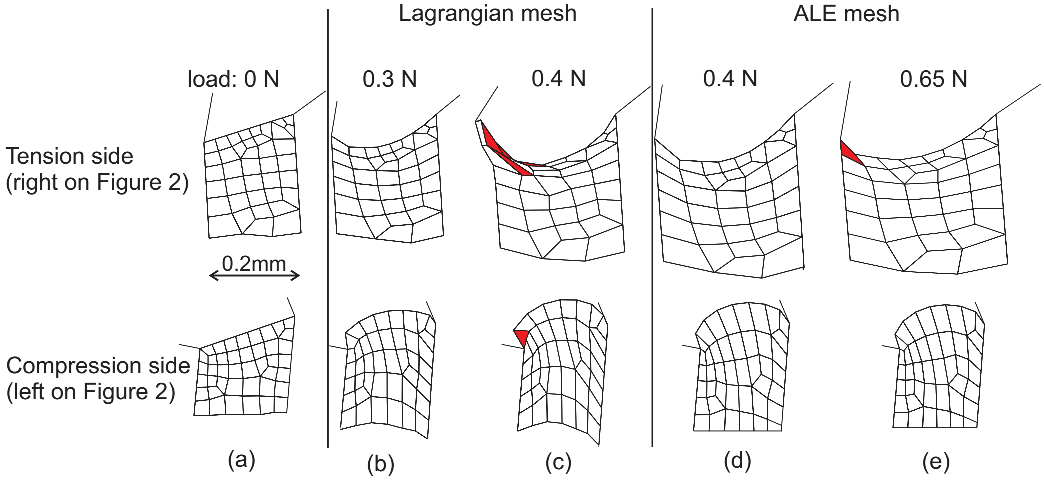

Figure 7: Zoom on the mesh evolution of the periodontal ligament at the alveolar margin. In red, the problematic elements.

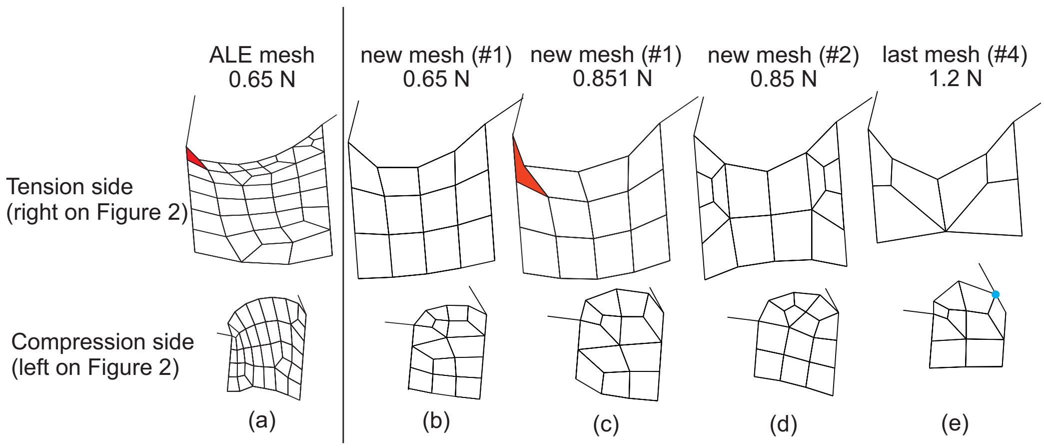

Figure 8: Zoom on the mesh of the periodontal ligament at the alveolar margin. In red, distorted elements (remeshing was required at those load values). In blue, node in contact with the base of the tooth crown.

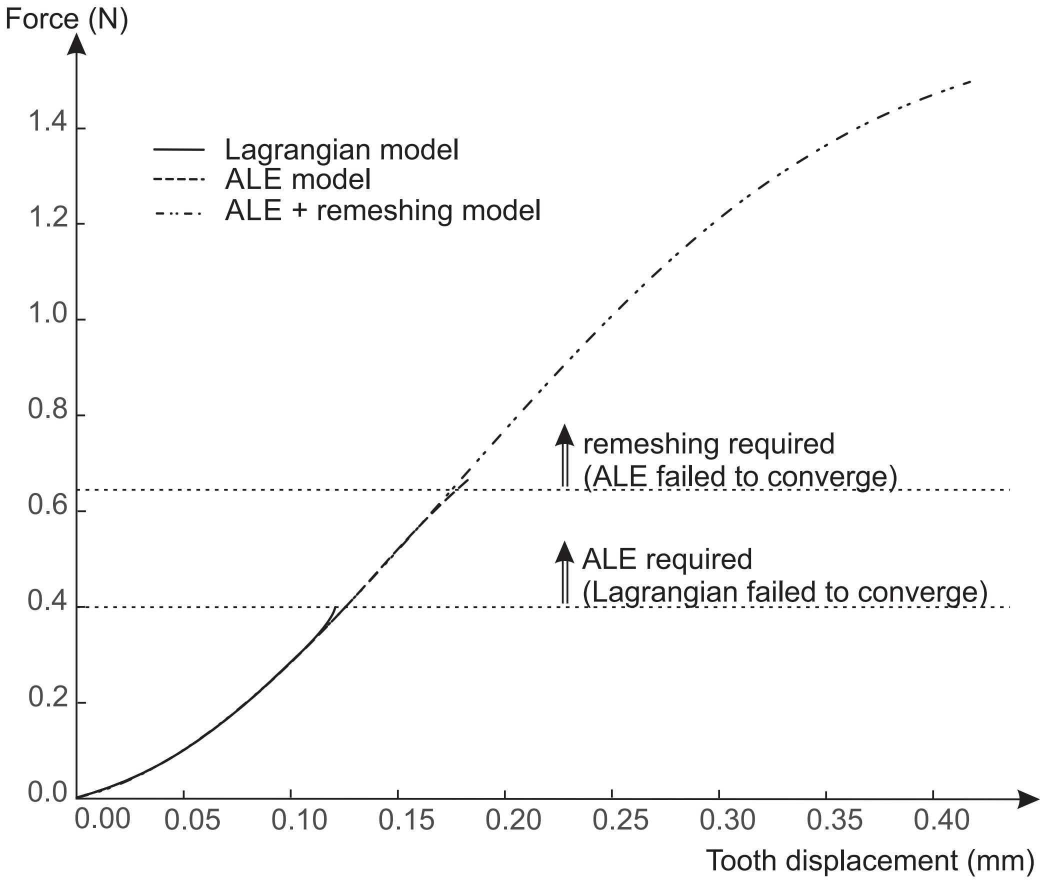

Figure 9: Force vs. tooth tip buccal displacement.